Langmuir

Article

pubs.acs.org/Langmuir

Sliding of Water Droplets on Smooth Hydrophobic Silane Coatings with Regular Triangle Hydrophilic Regions

Akira Nakajima,*[,†,‡] Yosuke Nakagawa,[†] Tsutomu Furuta,[†] Munetoshi Sakai,[‡] Toshihiro Isobe,[†] and Sachiko Matsushita[†]

[†]Department of Metallurgy and Ceramic Science, Graduate School of Science and Engineering, Tokyo Institute of Technology, 2-12-1 O-okayama, Meguro-ku, Tokyo 152-8552, Japan

[‡]Kanagawa Academy of Science and Technology, 308 East, Kanagawa Science Park 3-2-1 Sakado, Takatsu-ku, Kawasaki-shi, Kanagawa 213-0012, Japan

Supporting Information

ABSTRACT: The effect of the triangular pinning region on the sliding of water droplets on the smooth hydrophobic surface was investigated. Smooth hydrophobic silane coatings with various regular triangle hydrophilic regions were prepared using photolithography and octadecyltrimethoxysilane (ODS). The hydrophilic area in the surfaces was aligned hexagonally with a constant area fraction. Thereby water contact angles of the coatings were almost equivalent. The water droplet sliding velocity increased continuously with increasing pattern size. Anisotropic sliding velocity was observed on the surface, suggesting different pinning effects. The sliding motion of water droplets on the gradient surface with changing hydrophilic region size deflects against the downward direction. The deflection length depends on the direction of triangle hydrophilic regions and the initial sliding position. These results demonstrate that control of the sliding velocity while sustaining the static contact angle is feasible by designing the shape and alignment of chemical heterogeneity.

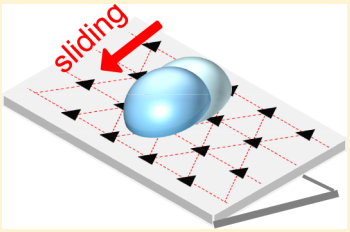

I. INTRODUCTION

In various industrial fields such as vehicle development, architecture, and electronics, the motion of a liquid droplet on a hydrophobic solid surface has been investigated frequently as an important subject for improved performance of water-repellent coatings. Hydrophobicity of solid surfaces is classifiable into two categories: static wettability and dynamic wettability.[1] The water contact angle is commonly measured as a criterion for evaluating static wettability. Although the sliding angle (the tilt angle at which the water droplet of a certain mass starts to slide down) and the contact angle hysteresis (the absolute value of the difference of cosines between advancing (θ_a) and receding (θ_r) contact angles) are often evaluated as criteria for assessing water-shedding properties of a hydrophobic surface,[2−6] they are not indexes of dynamic hydrophobicity, as are sliding acceleration and velocity, because they are thermodynamic properties and are not a function of time. Recognition of the importance of dynamic hydrophobicity is increasing gradually for assessment of the practical motion of water droplets on a solid surface. Several studies have been conducted using direct observations.[7−12]

Surface defects are well-known to affect water droplet motion and to increase the sliding angle and the contact angle hysteresis.[13] This phenomenon, commonly described as the "pinning effect",[14] is separable into two types.[15,16] The physical pinning effect originates from surface roughness. The chemical pinning effect results from chemical heterogeneity on the surface. Various studies of the pinning effect have been conducted to date.[17−31] However, because of the surface design difficulty or insufficient surface characterization, understanding of the respective contributions of these two pinning effects remains limited. Reportedly, the sliding behavior of water droplets is affected by the surface roughness, even of scale around 10 nm, when chemical heterogeneity is involved.[32] Therefore, highly physical homogeneity (average surface roughness (R_a) less than 1.0 nm) is regarded as necessary to decrease the contribution of physical pinning.

Various patterned coatings have been prepared using self-assembled monolayers (SAMs) and photolithography.[33−36] Very recently, we used photolithography to examine the effects of chemical pinning on the sliding behavior of the water droplets with avoidance of physical roughness on hexagonally patterned surfaces, which included homothetic hydrophilic areas of different sizes with smooth hydrophobic self-assembled monolayer coatings of a silane coupling agent (octadecyltrimethoxysilane (ODS)).[37] The results demonstrated that chemical surface defects provide different size dependence for sliding behavior between the critical moment at which a droplet slides down and the period when a droplet is sliding. It was deduced that the resistance against the droplet during sliding arises mainly from the interface between the ODS region and the hydrophilic region. The work was conducted using smooth hydrophobic ODS coatings with a circular hydrophilic area. The shape effect of the area has not been investigated. For this

Received: April 23, 2013
Revised: June 26, 2013
Published: June 26, 2013

study, we used photolithography to prepare three patterned surfaces with regular triangle hydrophilic areas of different sizes with a smooth ODS hydrophobic coating. Then the sliding velocity was evaluated from two directions. Moreover, we prepared gradient surface with different sizes of the hydrophilic regions. Using them, we investigated the sliding motion of water droplets on the surfaces. Then, the effect of the triangular chemical pinning region on sliding velocity was discussed.

II. EXPERIMENTAL SECTION

We used the same starting materials and substrates as those described for our earlier study.[37] The surface of a Si wafer washed using ethanol and acetone was precleaned using vacuum ultraviolet (VUV) light (λ = 172 nm with power density of around 7 mW cm^{-2}) irradiation for 30 min. Smooth hydrophobic coatings were obtained by heating the Si wafer with 20 μL of ODS in a Petri dish by flowing N_2 at 155 °C for 90 min. After rinsing, it was dried.

Chemically patterned coatings were prepared from the ODS coating using similar photomasks where equilateral-triangle-shaped holes (light-exposed area) were arranged in a regular hexagonal form. Figure 1 shows the pattern structure. Table 1 presents values of the

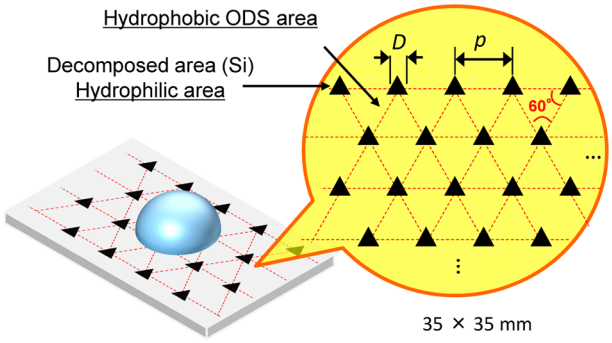

Figure 1. Schematic illustration of the hexagonal chemical pattern structure with triangle hydrophilic regions.

Table 1. Values of Triangle Side Size (D) and Pattern Distance (p) for Hexagonally Patterned Photomasks

pattern no.	1	2	3
square side size: D [μm]	6.8	13.5	27.0
pattern distance: p [μm]	15.0	30.0	60.0

side of the triangle (D) and pattern distance (p) at each photomask. The ratio of the light-exposed area to the total surface was 10%; it was constant for each photomask. Photoetching was conducted with VUV light irradiation in a vacuum condition (<50 Pa) for 10 min. The ODS placed under the light-exposed area of the photomask decomposed and became hydrophilic. A chemically patterned coating was obtained by rinsing with toluene and by subsequent drying.

We also prepared gradient surface with changing hydrophilic region size. Figure 2 presents a schematic illustration of the surface design. In this surface, the triangular hydrophilic region (1 mm width) decreased gradually (gradation rate between the regions: 0.95) from left to right while sustaining the light-exposed area to the total surface as 10%.

Water-based ink was applied to each chemically patterned coating. A hydrophilic area obtained through decomposition of the ODS coating was observed using an optical microscope (BX51TRF; Olympus Corp., Tokyo, Japan). Measurement conditions for surface roughness, contact angle, sliding angle, and sliding velocity were the same as those used in a previous study.[37] The droplet mass for contact angle measurements was 3.0 μL. That for sliding angle and sliding velocity measurements was 30 μL. In this study, the sliding velocity was measured at the coordinate of the advancing edge of the sliding droplet because no significant difference or delay was observed

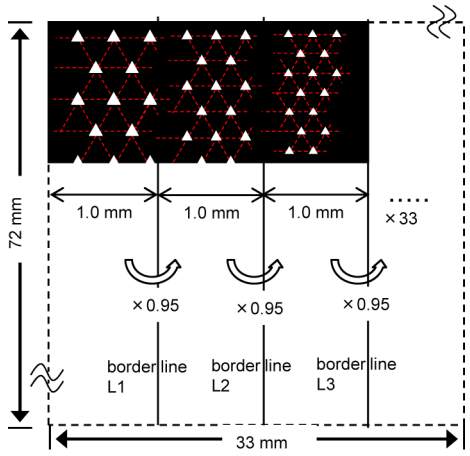

Figure 2. Schematic illustration of the designed graded surface with changing hydrophilic region size.

between advancing and receding edges during sliding (Supporting Information).

Moreover, we observed the motion of the triple-phase line (solid–liquid–air interface of the droplet on the surface) directly by withdrawal of the coatings from water. The coatings were immersed into water, then vertically withdrawn from the water using a commercial dip-coating system (ND-0407; Eintesla Inc., Tokyo, Japan) at a continuous rate (8 μm/s.). The motion of the triple-phase line was recorded using a CCD camera (DSA-100; A. KRÜSS Optronic GmbH, Hamburg, Germany). The experimental setup of this observation is depicted in Figure 3. Recorded images were converted into black and white images and were analyzed using Image-J software.

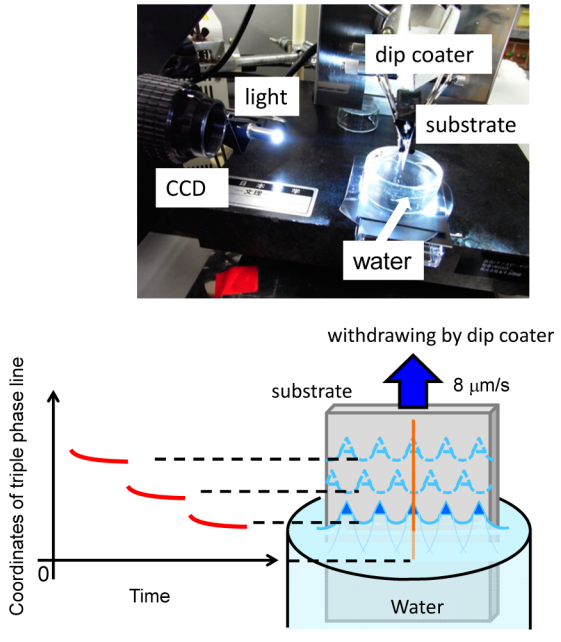

Figure 3. Experimental setup for direct observation of the triple-phase line motion.

III. RESULTS AND DISCUSSION

III-1. Chemically Patterned Coatings with Constant Hydrophilic Region Sizes. Figure 4a–c portrays optical microscope images of the obtained chemically patterned coatings with applied water-based ink. Results show that triangular chemical defects (hydrophilic area) were formed

dx.doi.org/10.1021/la401517v | Langmuir 2013, 29, 9269–9275

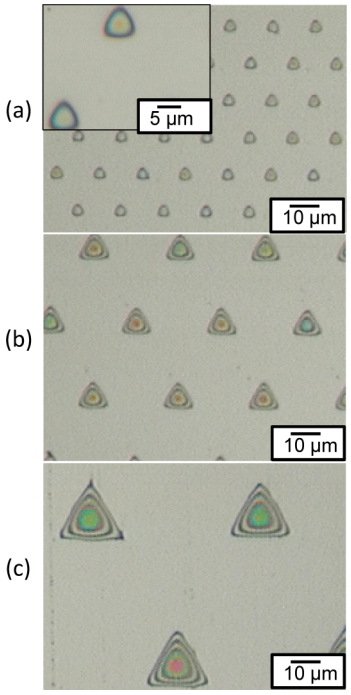

Figure 4. Optical microscope images of (a) pattern 1, (b) pattern 2, and (c) pattern 3 with applied water-based ink.

uniformly with regular hexagonal alignment. Differences in the shape and size of decomposed region were almost negligible. No particulate agglomerate was observed on these coatings using AFM. The surface roughness values (R_a) were the following: (a) pattern 1, 0.5 nm; (b) pattern 2, 0.6 nm; and (c) pattern 3, 0.5 nm. It is noteworthy that the R_a value of the plane ODS coating before photolithography was 0.2 nm. These coatings sustained nanolevel smoothness with suppression of physical roughness. The ODS chain length is a few nanometers. It is expected that ODS molecules are not standing vertically but are instead lying down or declining against the substrate on the surface after chemical vapor deposition treatment. Moreover, part of the decomposed area is expected to be included in the scanning area on this size relation. However, measurements at several different points yielded almost identical results. Therefore, we consider that the obtained coatings sustained nanolevel smoothness with suppression of physical roughness even though ODS molecules were decomposed using photolithography.

The chemically patterned coating surface can be defined as the compound surface of the ODS coating area (hydrophobic) and the decomposed area (hydrophilic). The practical contact angle values were 98 ± 1°, 97 ± 1°, and 98 ± 1°, respectively, for patterns 1, 2, and 3. The radii for 3.0 and 30 μL spherical droplets before contacting solid surface were, respectively, 0.89 and 1.93 mm. Assuming spherical cap geometry of the droplet and the flat surface, which provides a circular three-phase line, the radii of the contact circle for the surface with contact angle of 98° are calculable as 1.04 and 2.26 mm.[4] The chemical pattern is much smaller than that of a water droplet. Therefore, the composition ratio placed under the water contact area is expected to be equivalent to that on the triple-phase line. For that reason, we applied Cassie's model[38] for the obtained contact angle values as the first approximation. The contact angle on the compound surface of ODS coating and hydrophilic region by UV illumination (θ^*) can be described as

$$\cos\theta^* = f_{UV}\cos\theta_{UV} + (1 - f_{UV})\cos\theta_{ODS} \quad (1)$$

where f_{UV} signifies the area fractions (<1) of the hydrophilic region in the coating. In this equation, θ_{UV} and θ_{ODS} respectively denote the contact angle of the hydrophilic region and ODS coating. These values were obtained from experiments respectively as θ_{UV} = 22 ± 1° and θ_{ODS} = 104 ± 1°. It is noteworthy that immediately after UV illumination, the surface is highly hydrophilic, with θ_{UV} of less than 10°. However, this state is not stable. It is converted gradually to hydrophobic because of adsorption of gaseous organic molecules onto the surface with a high surface energy. If this condition is used for the experiment, then data scatter because of the influence of environmental condition in the laboratory. Therefore, we performed preliminary experiments for this research to investigate the relation between the storage time of the sample in the clean vessel after UV illumination and the contact angle. Results show that θ_{UV} becomes stable at around 22° by one week storage after UV illumination. Consequently, this experiment was conducted under this condition. The estimated area fraction of decomposed area (f_{UV}) is expected to be 0.1. The expected contact angle values for the chemically patterned coatings were calculated as 97.7°. The contact angle values (θ^*) were almost equivalent to each chemically patterned coating. These results imply that the designed chemical patterns were attained in the ODS coatings.

Figure 5 portrays the contact angle hysteresis values ($\Delta\cos\theta = |\cos\theta_a - \cos\theta_r|$) on each patterned coating when a water

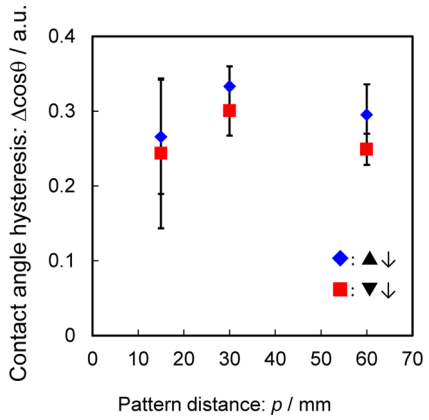

Figure 5. Pattern size dependence for contact angle hysteresis.

droplet started to slide down. In this study, the absolute value of the difference of cosine between advancing and receding contact angles is applied as the contact angle hysteresis because the force balance when a droplet commences sliding down on an inclined plate was discussed in this form by Furmidge.[2] The practical advancing and receding contact angle values were θ_A = 107.0 ± 0.7°, θ_R = 91.5 ± 3.8° (▲↓ pattern 1); θ_A = 104.0 ± 2.2°, θ_R = 89.9 ± 3.9° (▼↓ pattern 1); θ_A = 107.2 ± 1.2°, θ_R = 87.8 ± 2.3° (▲↓ pattern 2); θ_A = 107.5 ± 2.6°, θ_R = 90.0 ± 1.2° (▼↓ pattern 2); θ_A = 106.9 ± 3.1°, θ_R = 89.7 ± 0.6° (▲↓ pattern 3); and θ_A = 106.7 ± 0.6°, θ_R = 92.2 ± 0.7° (▼↓ pattern 3). In this explanation, ▲↓ means that the sliding direction is from the vertex to the base of the triangle; ▼↓ signifies the opposite direction. The corresponding sliding angle values were 16 ± 2° (▲↓ pattern 1), 14 ± 3° (▼↓ pattern 1), 18 ± 2° (▲↓ pattern 2), 16 ± 1° (▼↓ pattern 2), 14 ± 2° (▲↓ pattern 3), and 14 ± 1° (▼↓ pattern 3).

dx.doi.org/10.1021/la401517v | Langmuir 2013, 29, 9269−9275

Choi et al., after investigating the contact angle hysteresis of a highly hydrophobic surface with anisotropic roughness, proposed a revision of Cassie's equation using the differential area ratio instead of the simple surface area ratio.[39] For the experiments conducted for this study, the surface is smooth at the nanolevel. The physical surface roughness is negligible. The triangular hydrophilic area in the surfaces is aligned hexagonally with a constant area fraction. Therefore, differential area ratios are expected to be constant for these three surfaces when the sliding direction against the hydrophilic triangle area is the same. According to their study, the contact angle hysteresis is expected to be independent of the pattern size, and our experimentally obtained result corresponds with their study. However, in the former case of circular hydrophilic regions, the contact angle hysteresis increased concomitantly with increasing pattern distance.[37] It was deduced that a different mechanism originating from the hydrophilic region shape exists in the present case. The reason for this difference is discussed in the following section.

Figure 6 shows the relation between time and distance for water droplets during sliding to the ▼↓ direction on each

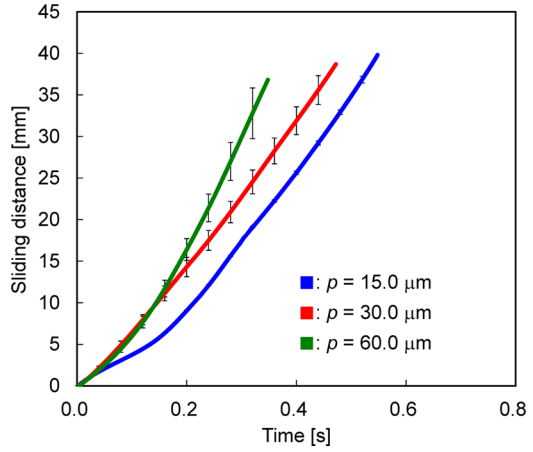

Figure 6. Sliding distance vs time for a water droplet: blue line, p = 15 μm; red line, p = 30 μm; and green line, p = 60 μm.

patterned coating inclined at 35°. Figure 7 depicts the relation between time and distance for water droplets during sliding to the ▼↓ and ▲↓ directions on the pattern 3 coating inclined at

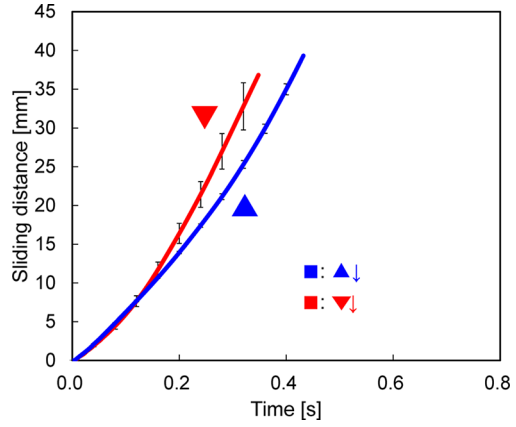

Figure 7. Sliding distance vs time for a water droplet on the pattern 3 surface: blue line, ▲↓ and red line, ▼↓.

35°. After conducting sliding velocity measurements three times for each condition, we obtained the average and standard deviation for each time. Figures 6 and 7 portray plots of the average and error bars for corresponding times and experimental conditions. The sliding velocity values increased concomitantly with increasing pattern distance. A similar trend was obtained from the sliding to the ▲↓ direction. These results imply that the moving resistance for water droplets during sliding decreases concomitantly with increasing pattern distance, and corresponds to the cases of circular hydrophilic regions.[37] As revealed in that earlier study, the resistance for the droplet motion arises mainly from the interface between the ODS region and the hydrophilic one. The sliding velocity of the ▼↓ direction is greater than that of the ▲↓ direction, which suggests that a difference in the sliding resistance exists between these two directions.

Figure 8 (movie is in the Supporting Information) presents results of direct observations obtained using a dip-coating

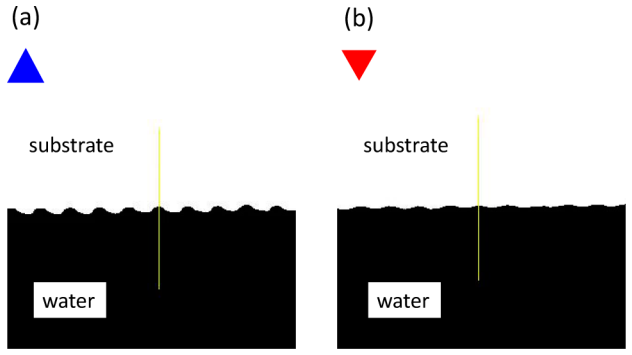

Figure 8. Black and white images of the triple-phase line during vertical withdrawal for the pattern 3 surface: (a) ▲↓ direction and (b) ▼↓ direction.

system. The coating was withdrawn to the ▲↓ (Figure 8a) and ▼↓ (Figure 8b, for which the withdrawal direction for both was the ↑) direction. The deflection of the triple-phase line is greater in the ▲↓ direction than in the ▼↓ direction. Figure 9a,b portray the relation between time and the top coordinate

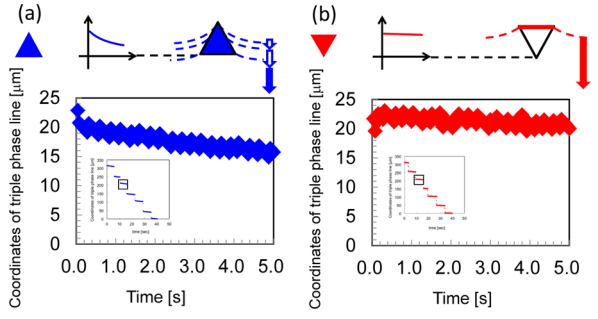

Figure 9. Movement of the triple-phase line on the pattern 3 surface: (a) ▲↓ direction and (b) ▼↓ direction. These are enlarged views of the region enclosed by the square of the inset figures.

of the triple-phase line in a triangular hydrophilic region. The coordinate is obtained at the intervals after and before the motion of the triple-phase line between different hydrophilic regions' lines. Coordinates of the triple-phase line decrease gradually in the ▲↓ direction, although they are constant in the ▼↓ direction. The moving triple-phase line in the ODS

dx.doi.org/10.1021/la401517v | Langmuir 2013, 29, 9269−9275

coatings encounters resistance once it meets the hydrophilic region. The degree of the resistance is expected to be the maximum when the line is parallel to the side of the triangle. Once the driving force exceeds the maximum resistance, the line moves immediately to the next hydrophilic region. This is the motion in the ▼↓ direction (upper panel in Figure 9b). Therefore, the top coordinate of the triple-phase line is constant during pinning. However, the degree of the resistance, which is initially small, increases gradually to the maximum when the line meets from the vertex of the triangle (upper panel in Figure 9a). Therefore, the top coordinate of the triple-phase line also decreases gradually during pinning. These results imply that the entire area of each triangle contributes sliding resistance in the sliding to the ▲↓ direction. However, only the top side of each triangle provides sliding resistance in the sliding to the ▼↓ direction. The entire resistance for the motion of the triple-phase line is expected to be greater in the ▲↓ direction than in the ▼↓ direction, which corresponds to anisotropy of the sliding velocity. This characteristic is unique for the triangular hydrophilic region shape.

Based on research by Choi et al.,[39] the differential area ratio differs between ▼↓ and ▲↓ directions. The former gradually decreases the hydrophilic region in the line of the triangle and the latter increases. However, differences for the practical advancing and receding contact angles between ▼↓ and ▲↓ directions are not remarkable. The motion difference of the three-phase line between ▼↓ and ▲↓ directions by dip-coater was distinct. The average value of the contact angle hysteresis for the▲↓ direction seems slightly greater than that for the ▼↓ direction. The degree of the difference might depend on the tilt angle or motion velocity.

When the sliding distance was greater than about 10 mm, effects of vibration at the instant of droplet departure from the pipet become small. The droplet seems to slide down by constant velocity in Figure 6. The velocity was calculated as 86.3 (for pattern 1), 89.6 (for pattern 2), and 139.4 mm/s (for pattern 3) in this region. The motion energy of the droplet calculated from these velocities was a few percent of the potential energy because of the energy dissipation. In this study, the contact angle change during velocity measurement was quite small and almost negligible, suggesting constant hydrostatic pressure in the contact area. Flowing resistance is expected to be provided from the hydrophilic area. However, their area fraction is the same in this study. Based on a previous study of the relation between contact area and moving resistance,[40] the same flowing resistance from the hydrophilic area is expected for all surfaces. Therefore, we infer that viscous dissipation attributable to the no-slip boundary conditions is the same, and that the main reason for the difference in energy dissipation is pinning, as discussed in our previous study[37] because it depends on the practical interface amount and depends inversely on the pattern size.

III-2. Chemically Patterned Coatings with Size Gradation. Figure 10 shows optical microscope images of obtained chemically patterned coatings. The water contact angle of the gradient surfaces was 97 ± 1°, suggesting a 10% hydrophilic region ratio as designed. We evaluated the sliding behavior of water droplets from two directions to compare ▲↓ and ▼↓ directions (Figure 11). Figure 12 shows sequential top-view images of the outline of a 35-μL water droplet sliding on the gradient surface. When a droplet slid down in the ▲↓ direction, its trajectory deflected to the right against the downward (orange arrow in Figure 12b) direction. An opposite

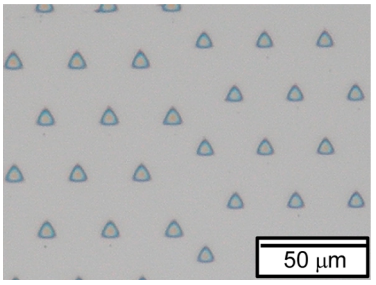

Figure 10. Optical microscope images of gradient surface with changing hydrophilic region size.

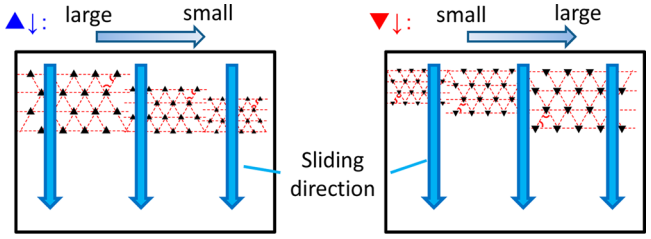

Figure 11. Sliding behavior evaluation of water droplets on the graded surface from two directions.

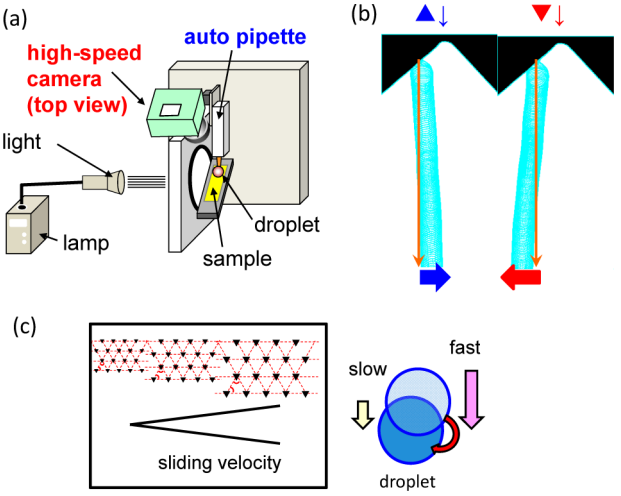

Figure 12. (a) Schematic illustration of the top-view observation apparatus for water droplets on graded surfaces. (b) Sequential top-view images of the outline of a 30-μL water droplet sliding on a graded surface. (c) Schematic illustration of the sliding velocity difference for water droplets on graded surfaces.

trend was observed when a droplet slid down in the ▼↓ direction. In this study, we define "deflection length" as the absolute displacement to right or left from the top view when the droplet slides down for 4 cm length from the side view on the surface declined at 35°. The deflection length was greater for the ▼↓ direction than the ▲↓ direction (Figure 12b). Assuming that the resistance for the droplet motion arises mainly from the solid–liquid interface,[37] the length of the interface contained per unit area (ϕ_{IL}) for the coatings in this study can be described as

$$\varphi_{IL} = \frac{3D}{(1/2)p^2 \sin 60^\circ} \quad (2)$$

Therefore, when the pattern size becomes n times, the value of ϕ_{IL} becomes $1/n$ (because of the linear relation between D

dx.doi.org/10.1021/la401517v | Langmuir 2013, 29, 9269–9275

and p). When ϕ_{IL} increases concomitantly with decreasing pattern size (p), it is expected that the sliding velocity decreases gradually. The contact radius of the droplet in this study was 3−5 mm, and the sliding droplet always ranges at least a few areas with different pattern sizes. Consequently, the velocity difference is induced in the sliding droplet and its trajectory is deflected to the direction of smaller pattern size (Figure 12c). Figure 13 presents schematic illustrations for the triple-phase

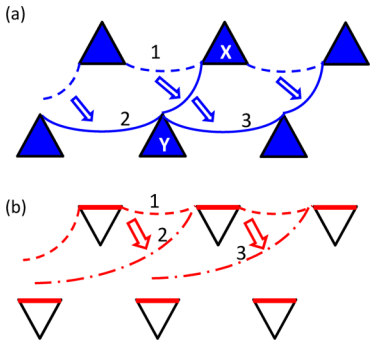

Figure 13. Anisotropy of deflection length caused by the pinning effect by triangle hydrophilic area: (a) ▲↓ direction and (b) ▼↓ direction. Inset figures show motion of the triple-phase line observed using a dip-coater system during vertical withdrawal.

line motion for the ▲↓ and ▼↓ directions. This figure is presented to show the left-to-right motion of the line. For the ▲↓ direction, the triple-phase line moves from 1 to 3. During this process, the line reaches the oblique side of the triangle (X in the figure); then it moves to the vertex of the triangle (Y). In this motion, the line meets moving resistance from the oblique side of the triangle in X. For the ▼↓ direction, the triple-phase line moves without meeting the triangle side. Once the driving force exceeds the maximum resistance from the side of the triangle, the line moves immediately to the next hydrophilic region. Therefore, the side motion from 1 to 3 is expected to be smoother than that in the ▲↓ direction. Consequently, the deflection length was greater for the ▼↓ direction than the ▲↓ direction. The motion of the triple-phase line on the hydrophobic coating with regular triangle hydrophilic region is complex (similar motion of the triple-phase line was also observed during evaporation (Supporting Information movie)). The small pattern distance dependency in contact angle hysteresis might also be attributable to this complex motion anisotropy.

It is noteworthy that the deflection length depends on the initial sliding position (Figure 14). The deflection length when the droplet slides down from a large pattern region is greater than that when it slides down from a small pattern region. Although a constant homothetic ratio is retained between neighboring pattern region for the gradient surface, the absolute value of pattern size difference between them is not constant. When the pattern size decreases, the absolute value of pattern size difference decreases. The droplet size is constant. Therefore, the pattern size difference between the right and left sides of the droplet is small when the pattern size is small. This difference causes differences of the deflection length because it is an origin of the velocity difference for the right and left side of the droplet.

This deflection trend during sliding was not observed for a hexane droplet (Figure 15). This effect is expected to be less remarkable when the wettability difference between the ODS

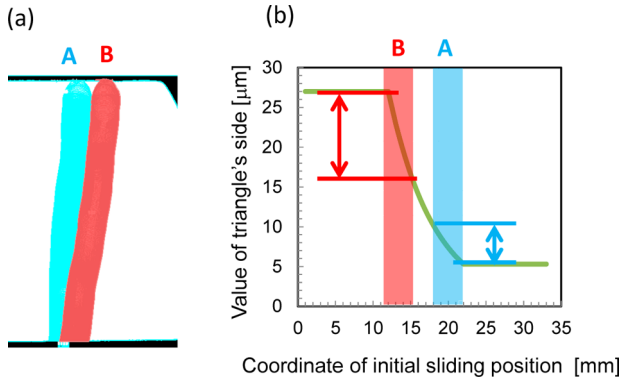

Figure 14. Initial sliding position dependence of the deflection length: (a) sequential top-view images of the sliding droplets from two positions (A and B) to the ▼↓ direction; (b) practical side length range of the triangle for position A and position B.

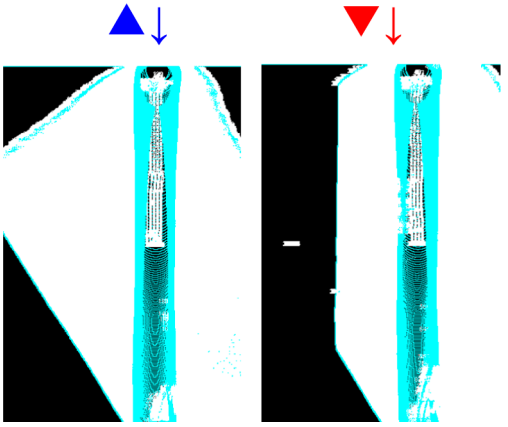

Figure 15. Sequential top-view images of the outline of a 30-μL hexane droplet sliding on a graded surface.

coating and the triangle hydrophilic region is small. Hexane is a nonpolar solvent with low surface energy (18.4 mJ/m^2 at 20 °C).[41] Therefore, it merely spread and did not deflect on the surface.

This study was conducted only for a well-defined triangular chemically patterned coating. Effects of the defect distribution (shape and direction) cannot be discussed based on results of this study. These topics will be addressed in future work.

IV. CONCLUSION

For this study, we used photolithography to prepare three patterned surfaces with triangular hydrophilic areas of different sizes, each with a smooth ODS hydrophobic coating. The hydrophilic area in the surfaces was aligned hexagonally with a constant area fraction. The surface was smooth at the nanolevel: physical surface roughness was negligible. The water droplet sliding velocity increased concomitantly with increasing pattern size and exhibited anisotropy. The sliding motion trajectory of water droplets on the gradient surface with changing hydrophilic regions size deflects against the downward direction. The deflection length depends on the direction of triangle hydrophilic regions and the initial sliding position. These results demonstrate that control of the sliding velocity with a sustained static contact angle is feasible by designing the shape and alignment of chemical heterogeneity and that

dx.doi.org/10.1021/la401517v | Langmuir 2013, 29, 9269−9275

manipulation of sliding behavior for water droplets can be achieved through proper control of these effects.

■ ASSOCIATED CONTENT

Supporting Information

Additional material as discussed in the text. This material is available free of charge via the Internet at http://pubs.acs.org.

■ AUTHOR INFORMATION

Corresponding Author

*Tel.: +81-3-5734-2524. Fax: +81-3-5734-3355. E-mail: anakajim@ceram.titech.ac.jp.

Notes

The authors declare no competing financial interest.

■ REFERENCES

(1) Nakajima, A. Design of hydrophobic surfaces for the control of liquid droplets. *NPG Asia Mater.* **2011**, *3*, 49−56.

(2) Furmidge, C. G. L. The sliding of liquid drops on solid surfaces and a theory for spray retention. *J. Colloid Sci.* **1962**, *17*, 309−324.

(3) Carre, A.; Shanahan, M. E. R. Drop motion on an inclined plane and evaluation of hydrophobic treatments to glass. *J. Adhes.* **1995**, *49*, 177−185.

(4) Miwa, M.; Fujishima, A.; Nakajima, A.; Hashimoto, K.; Watanabe, T. Effects of the surface roughness on sliding angles of water droplets on super-hydrophobic surfaces. *Langmuir* **2000**, *16*, 5754−5760.

(5) Yoshimitsu, Z.; Nakajima, A.; Watanabe, T.; Hashimoto, K. Effect of surface structure on the hydrophobicity and sliding behavior of water droplets. *Langmuir* **2002**, *18*, 5818−5822.

(6) Zhang, X.; Cai, Y.; Mi, Y. Anisotropic wetting on checkerboard-patterned surface. *Langmuir* **2011**, *27*, 9630−9637.

(7) Durbin, P. A. Considerations on the moving contact-line singularity, with application to frictional drag on a slender drop. *J. Fluid Mech.* **1988**, *197*, 157−169.

(8) Richard, D.; Quere, D. Viscous drops rolling on a tilted non-wettable solid. *Europhys. Lett.* **1999**, *48*, 286−291.

(9) Podgorski, T.; Flesselles, J.-M.; Limat, L. Corners, cusps, and pearls in running drops. *Phys. Rev. Lett.* **2001**, *87*, 036102−1−4.

(10) Schwartz, L. W.; Roux, D.; Cooper-White, J. On the shapes of droplets that are sliding on a vertical wall. *Physica D* **2005**, *209*, 236−244.

(11) Yoshida, N.; Abe, Y.; Shigeta, H.; Nakajima, A.; Ohsaki, H.; Hashimoto, K.; Watanabe, T. Sliding behavior of water droplets on flat polymer surface. *J. Am. Chem. Soc.* **2006**, *128*, 743−747.

(12) Sakai, M.; Song, J.-H.; Yoshida, N.; Suzuki, S.; Kameshima, Y.; Nakajima, A. Direct observation of internal fluidity in a water droplet during sliding on hydrophobic surfaces. *Langmuir* **2006**, *22*, 4906−4909.

(13) Dettre, R. H.; Johnson, R. E., Jr. Contact angle, Wettability and Adhesion. *Advances in Chemistry Series*; American Chemical Society: Washington, DC, 1964; Vol. 43, pp 136−144.

(14) Quéré, D. Non-sticking drops. *Rep. Prog. Phys.* **2005**, *68*, 2495−2532.

(15) Johnson, R. E., Jr.; Dettre, R. H. *Surface and Colloid Science*; Matijevic, E., Ed.; Wiley-Interscience: New York, 1969; Vol. 2, pp 85−153.

(16) Decker, E. L.; Garoff, S. Contact line structure and dynamics on surfaces with contact angle hysteresis. *Langmuir* **1997**, *13*, 6321−6332.

(17) Dussan, E. B.; Chow, R. T. P. On the ability of drops or bubbles to stick to non-horizontal surfaces of solids. *J. Fluid Mech.* **1983**, *137*, 1−29.

(18) Youngblood, J. P.; MacCarthy, T. J. Ultrahydrophobic Polymer Surfaces Prepared by Simultaneous Ablation of Polypropylene and Sputtering of Poly(tetrafluoroethylene) Using Radio Frequency Plasma. *Macromolecules* **1999**, *32*, 6800−6806.

(19) Öner, D.; McCarthy, T. J. Ultrahydrophobic surfaces. Effects of topography length scales on wettability. *Langmuir* **2000**, *16*, 7777−7782.

(20) Buehrle, J.; Herminghaus, S.; Mugele, F. Impact of line tension on the equilibrium shape of liquid droplets on patterned substrates. *Langmuir* **2002**, *18*, 9771−9777.

(21) Iliev, S. D.; Pesheva, N. C. Wetting properties of well-structured heterogeneous substrates. *Langmuir* **2003**, *19*, 9923−9931.

(22) Ramos, S. M. M.; Charlaix, E.; Benyagoub, A. Contact angle hysteresis on nano-structured surfaces. *Surf. Sci.* **2003**, *540*, 355−362.

(23) Cubaud, T.; Fermigier, M. Advancing contact lines on chemically patterned surfaces. *J. Colloid Interface Sci.* **2004**, *269*, 171−177.

(24) Kusumaatmaja, H.; Leopoldes, J.; Dupuis, A.; Yeomans, J. M. Drop dynamics on chemically patterned surfaces. *Europhys. Lett.* **2006**, *73*, 740−746.

(25) Reyssat, M.; Quéré, D. Contact angle hysteresis generated by strong dilute defects. *J. Phys. Chem. B* **2009**, *113*, 3906−3909.

(26) Lv, C.; Yang, C.; Hao, P.; He, F.; Zheng, Q. Sliding of water droplets on microstructured hydrophobic surfaces. *Langmuir* **2010**, *26*, 8704−8708.

(27) Bormashenko, E.; Musin, A.; Zinigrad, M. Evaporation of droplets on strongly and weakly pinning surfaces and dynamics of the triple line. *Colloid Surf. A* **2011**, *385*, 235−240.

(28) Urata, C.; Masheder, B.; Cheng, D. F.; Hozumi, A. How to reduce resistance to movement of alkane liquid drops across tilted surfaces without relying on surface roughening and perfluorination. *Langmuir* **2012**, *28*, 17681−17689.

(29) Pilat, D. W.; Papadopoulos, P.; Schaffel, D.; Vollmer, D.; Berger, R.; Butt, H. J. Dynamic measurement of the force required to move a liquid drop on a solid surface. *Langmuir* **2012**, *28*, 16812−16820.

(30) Hong, S. J.; Chang, C. C.; Chou, T. H.; Sheng, Y. J.; Tsao, H. K. A drop pinned by a designed patch on a tilted superhydrophobic surface: mimicking desert beetle. *J. Phys. Chem. C* **2012**, *116*, 26487−26495.

(31) Luo, L. X.; Gupta, R.; Frechette, J. Modulating contact angle hysteresis to direct fluid droplets along a homogeneous surface. *ACS Appl. Mater. Int.* **2012**, *4*, 890−896.

(32) Furuta, T.; Nakajima, A.; Sakai, M.; Kameshima, Y.; Okada, K. Evaporation and sliding of water droplets on fluoroalkylsilane coatings with nanoscale roughness. *Langmuir* **2009**, *25*, 5417−5420.

(33) Sugimura, H.; Ushiyama, K.; Hozumi, A.; Takai, O. Micro-patterning of alkyl- and fluoroalkylsilane self-assembled monolayers using vacuum ultraviolet light. *Langmuir* **2000**, *16*, 885−888.

(34) Koga, T.; Morita, M.; Ishida, H.; Yakabe, H.; Sasaki, S.; Sakata, O.; Otsuka, H.; Takahara, A. Dependence of the molecular aggregation state of octadecylsiloxane monolayers on preparation methods. *Langmuir* **2005**, *21*, 905−910.

(35) Morita, M.; Koga, T.; Otsuka, H.; Takahara, A. Macroscopic-wetting anisotropy on the line-patterned surface of fluoroalkylsilane monolayers. *Langmuir* **2005**, *21*, 911−918.

(36) Suzuki, S.; Nakajima, A.; Tanaka, K.; Sakai, M.; Hashimoto, A.; Yoshida, N.; Kameshima, Y.; Okada, K. Sliding behavior of water droplets on line-patterned hydrophobic surfaces. *Appl. Surf. Sci.* **2008**, *254*, 1797−1805.

(37) Furuta, T.; Sakai, M.; Isobe, T.; Matsushita, S.; Nakajima, A. Sliding of water droplets on hydrophobic surfaces with various hydrophilic region sizes. *Langmuir* **2011**, *27*, 7307−7313.

(38) Cassie, A. B. D. Contact angles. *Discuss. Faraday Soc.* **1948**, *3*, 11−16.

(39) Choi, W.; Tuteja, A.; Mabry, J. M.; Cohen, R. E.; McKinley, G. H. A modified Cassie−Baxter relationship to explain contact angle hysteresis and anisotropy on non-wetting textured surface. *J. Colloid Interface Sci.* **2009**, *339*, 208−216.

(40) Sakai, M.; Kono, H.; Nakajima, A.; Zhang, X.; Sakai, H.; Abe, M.; Fujishima, A. Sliding of water droplets on the superhydrophobic surface with ZnO nanorods. *Langmuir* **2009**, *25*, 14182−14186.

(41) Dean, J. A. *Lange's Handbook of Chemistry*; McGraw-Hill Book Company: New York, 1979; pp 10−110.